

Geophysical Research Letters[®]

RESEARCH LETTER

10.1029/2021GL097047

Key Points:

- Sea ice predictability in the Weddell Sea is strongly determined by temperature and salinity profiles of the underlying upper ocean
- Every winter, the timing of the loss of sea ice predictability is defined when deep water is entrained into the mixed layer
- Sea ice predictability depends not only on the depth of the Winter Water layer but also on how strongly stratified its base is

Supporting Information:

Supporting Information may be found in the online version of this article.

Correspondence to:

S. Libera,
stephy.libera@utas.edu.au

Citation:

Libera, S., Hobbs, W., Klocker, A., Meyer, A., & Matear, R. (2022). Ocean-sea ice processes and their role in multi-month predictability of Antarctic sea ice. *Geophysical Research Letters*, 49, e2021GL097047. <https://doi.org/10.1029/2021GL097047>

Received 16 NOV 2021

Accepted 14 APR 2022

Author Contributions:

Conceptualization: Will Hobbs, Andreas Klocker, Amelie Meyer

Formal analysis: Stephy Libera, Will Hobbs, Andreas Klocker, Amelie Meyer, Richard Matear

Funding acquisition: Will Hobbs, Richard Matear

Investigation: Stephy Libera, Will Hobbs, Andreas Klocker, Amelie Meyer

Methodology: Stephy Libera, Will Hobbs, Andreas Klocker, Amelie Meyer

Resources: Will Hobbs

Software: Stephy Libera

© 2022. The Authors.

This is an open access article under the terms of the [Creative Commons Attribution-NonCommercial-NoDerivs License](https://creativecommons.org/licenses/by/4.0/), which permits use and distribution in any medium, provided the original work is properly cited, the use is non-commercial and no modifications or adaptations are made.

Ocean-Sea Ice Processes and Their Role in Multi-Month Predictability of Antarctic Sea Ice

Stephy Libera^{1,2} , Will Hobbs^{2,3} , Andreas Klocker⁴ , Amelie Meyer^{1,2} , and Richard Matear⁵ 

¹Institute for Marine and Antarctic Studies, University of Tasmania, Hobart, TAS, Australia, ²Australian Research Council Centre of Excellence for Climate Extremes, Sydney, NSW, Australia, ³Australian Antarctic Program Partnership, Institute for Marine and Antarctic Studies, University of Tasmania, Hobart, TAS, Australia, ⁴Department of Geosciences, University of Oslo, Oslo, Norway, ⁵CSIRO Oceans and Atmosphere, Hobart, TAS, Australia

Abstract Antarctic sea ice is a critical component of the climate system and a vital habitat for Southern Ocean ecosystems. Understanding the underlying physical processes and improving Antarctic sea ice prediction is of broad interest. Using the model data, we investigate sea ice and upper ocean predictability at interannual timescales in the Weddell Sea region. We find that oceanic predictability is largely confined to the Winter Water layer and responds to seasonal modifications of the water column, mainly driven by sea ice processes. Predictability depends not only on the depth of the Winter Water layer, but also on how strongly stratified its base is. Predictability is lost when warm Circumpolar Deep Water with no sea ice-related memory entrains into the mixed layer. We show the strong dependence of sea ice predictability on the local upper ocean vertical structure, which suggests that both are likely to change in a warming climate.

Plain Language Summary Antarctic sea ice is a critical component of climate and a vital habitat for Southern Ocean ecosystems. Therefore, understanding the drivers and physical processes influencing Antarctic sea ice, and being able to predict Antarctic sea ice is of broad interest. We assess the predictability of sea ice and underlying upper ocean in the Weddell Sea region of the Southern Ocean using the model data. We find that sea ice processes influence the upper ocean temperature, and these thermal signatures linger in the ocean producing sea ice predictability over multiple months. Here, we show that the oceanic memory in the upper ocean is largely found within the Winter Water layer (i.e., cold water layer formed during sea ice formation). Oceanic memory and sea ice predictability are suddenly lost when warm deep waters from the ocean interior entrain into the surface mixed layer in mid-winter. This limit to sea ice predictability has not been explored before, and it shows the strong dependency of sea ice predictability in a region to its local vertical structure of oceanic properties and their seasonal evolution. This implies that changes to upper ocean properties in a warming climate can likely alter the sea ice predictability patterns in the future.

1. Introduction

The growth and melt of Antarctic sea ice, arguably the strongest seasonal cycle on the planet (Handcock & Raphael, 2020), affects global climate through its interplay with planetary albedo, atmospheric circulation, thermohaline circulation, and ocean productivity (Abernathey et al., 2016; Brandt et al., 2005; Hobbs et al., 2016; Massom & Stammerjohn, 2010; Raphael & Hobbs, 2014). The close interaction of Antarctic sea ice with the ocean and atmosphere has been linked to interannual variability and trends in sea ice (Hobbs et al., 2016; Holland, 2014; Lecomte et al., 2017; Martinson, 1990). Antarctic sea ice predictability studies have identified the strong dependence of sea ice predictability on oceanic processes, pointing toward sea ice-ocean interactions (M. M. Holland et al., 2013; Marchi et al., 2019; Ordoñez et al., 2018; Zunz et al., 2015). This study aims to better understand the physical processes in the ocean associated with sea ice predictability.

Sea ice predictability studies are diverse, with predictions ranging from seasonal to decadal timescales, using statistical or dynamical approaches and based on observations or climate model data. They have a variety of applications ranging from planning operational activities (scientific research, tourism, shipping, fisheries management, and conservation) to evaluating climate projections and policy decision-making (Blanchard-Wrigglesworth et al., 2011; Bushuk et al., 2021; Chen & Yuan, 2004; Giese et al., 2021; Guemas et al., 2016; M. M. Holland et al., 2013; Juricke et al., 2014; Kearney et al., 2021; Marchi et al., 2019, 2020; Massonnet et al., 2019; Ordoñez et al., 2018; Yang et al., 2016; Zampieri et al., 2019; Zunz et al., 2015). In this study, we evaluate sea ice

Supervision: Will Hobbs, Andreas Klockner, Amelie Meyer, Richard Matear
Validation: Will Hobbs
Visualization: Stephy Libera, Andreas Klockner, Amelie Meyer, Richard Matear
Writing – original draft: Stephy Libera
Writing – review & editing: Stephy Libera, Will Hobbs, Andreas Klockner, Amelie Meyer, Richard Matear

and ocean predictability at seasonal to interannual timescales in the Weddell sector (Figure 1a). We use lagged correlations to evaluate the inherent memory of the ice-ocean system in a forward-looking perspective of predictability, that is, indicating how a given initial state is retained in the system and continues to influence the future states. There may be external sources of predictability from atmospheric forcings, for example, ENSO effects (Simpkins et al., 2012) that we do not consider in this study. In the Southern Ocean, the Weddell Sea is one of the dominant regions of sea ice production. Its geographical setting limits dynamical influence from advected oceanic and sea ice properties into this region, making it ideal for studying local ice-ocean interaction.

Previous studies have established the link between the upper ocean heat content (OHC) and sea ice predictability (M. M. Holland et al., 2013; Marchi et al., 2019). These studies found that sea ice predictability can persist for some months but is then generally lost during the ice-retreat season before reemerging in the following ice-growth season. Marchi et al. (2019) calculated the predictability of integrated OHC in the upper 100 m and showed strong correspondence between regions of high sea ice predictability and oceanic predictability. When integrating the OHC as done by Marchi et al. (2019), information about the evolution of heat anomalies in the vertical oceanic layers is lost, and this limits our capacity to observe the physical process occurring within the ocean.

In this study, we retain the vertical dimension for oceanic predictability results and compare the evolution of predictability of sea ice and ocean simultaneously. We find the loss of predictability in summer followed by the reemergence of predictability in autumn consistent with M. M. Holland et al. (2013) and Marchi et al. (2019). We also find a sudden loss of predictability in mid-winter when warm Circumpolar Deep Water is entrained into the mixed layer, connecting the influence of local vertical ocean structure and sea ice processes. These findings not only give insights into the physical processes in the upper ocean underlying sea ice predictability, but also direct toward hydrographic features that are valuable for understanding the regional differences in Antarctic sea ice trends and variability.

2. Methods

2.1. Data

We use the outputs from a global coupled ocean-sea ice model, the Australian Community Climate and Earth System Simulator (ACCESS-OM2) (ACCESS-OM2; Kiss et al., 2020). ACCESS-OM2 is based on the ocean MOM5.1 and ice CICE5.1 models coupled with the OASIS-MCT coupler. The model experiment analyzed in this study was forced using JRA55-do v1.4.0 (Tsujino et al., 2018). The high horizontal resolution of 0.1° in ACCESS-OM2-01 produces a good representation of Southern Ocean dynamics and adequate simulations of the Antarctic sea ice extent and concentration: The mean annual cycle of Antarctic sea ice extent from ACCESS-OM2-01 closely matches observations, and the historical sea ice trends are also well represented (Kiss et al., 2020).

To calculate the observed sea ice area (SIA) used in this study, we use the sea ice concentration (SIC) derived from satellite passive microwave data (a product based on the NASA Goddard-merged parameter in the NOAA/NSIDC Climate Data Record [CDR]) (Meier et al., 2013).

2.2. Correlation Analysis and Statistical Methods

In our diagnostic predictability analysis, we calculate the correlation between a given initial month and the 12 future months using monthly data from 1985 to 2015 (hereafter correlation analysis). For the SIA, we calculate the total SIA in the Weddell sector, create the monthly time series, and detrend it by subtracting the linear least squares fit, then we apply the correlation analysis (hereafter referred to as “sea ice predictability”). To evaluate the predictability of the ocean from its initial state, we calculate spatial averages within the oceanic area between 90°S and winter sea ice extent maximum (from the model) for the Weddell Sea region approximated at 58°S. Spatial averaging for conservative temperature (T) produces time series of vertical profiles in the upper 200 m. These time series are detrended before applying the correlation analysis (T from the initial month correlated with future T at the same depth), hereafter referred as “ocean-ocean correlations.” Then using the detrended monthly time series of total SIA and T in the upper 200 m, we calculate correlations between given initial SIA with future T at depth, to investigate the signature of ice-ocean interactions (hereafter referred to as “ice-ocean correlation”). We define statistically significant values as p -values greater than 95% in the two-tailed Student's T -test.

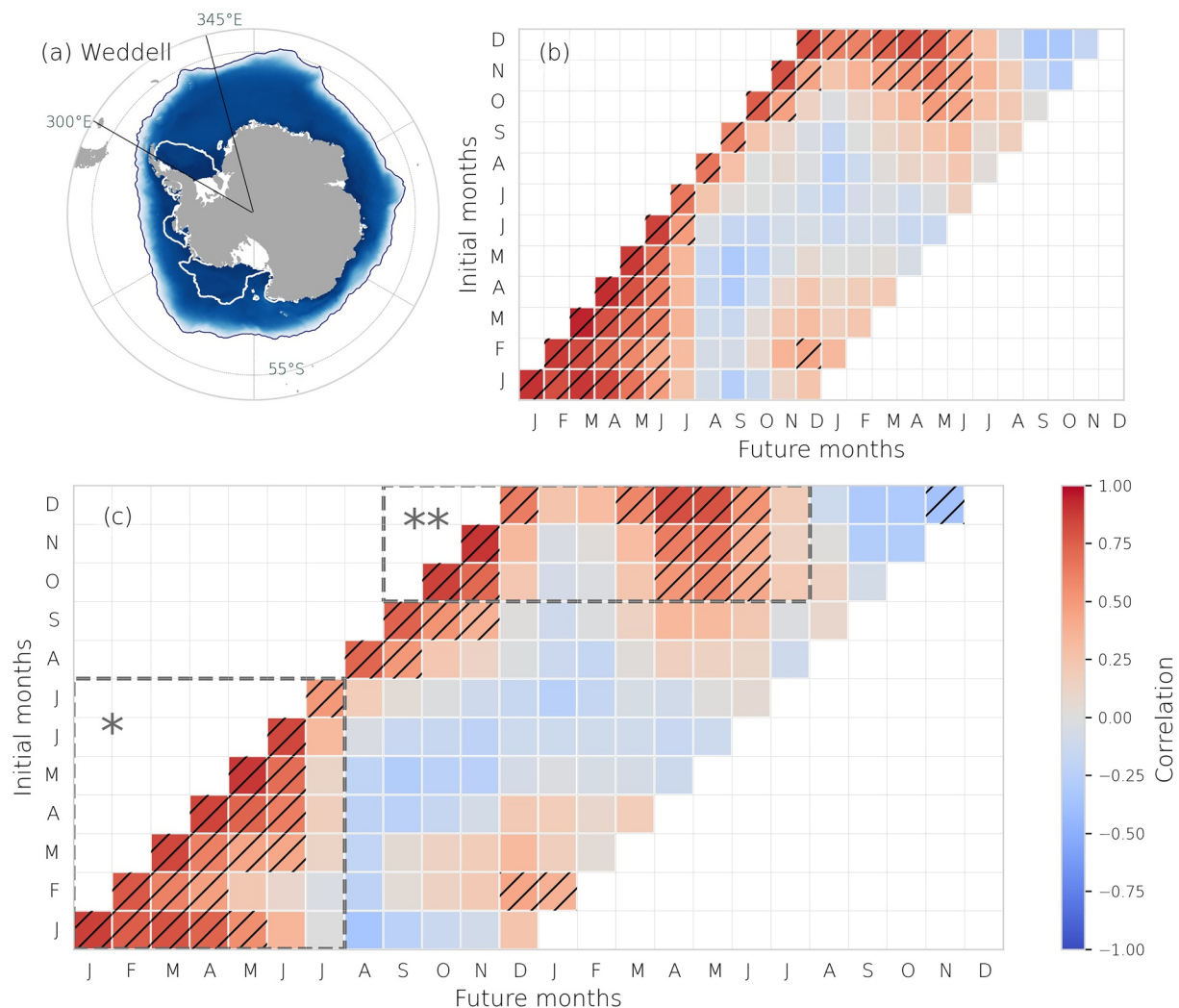


Figure 1. (a) Map defining the Weddell sector in Antarctica along with the model climatological winter maximum (September) of sea ice extent (in shading) and summer minimum (February, white contour); (b) sea ice predictability, autocorrelation of sea ice area (SIA) from observation; and (c) sea ice predictability from model output. In (b) and (c), SIA from initial months (or lead) along the y axis are correlated against the SIA in the future months (or lags) along the x axis and statistically significant values (>95%) are hatched. Summer persistence (*) and spring reemergence (**) patterns are marked in (c).

2.3. Climatology

To understand the general ice and ocean seasonal evolution in the Weddell sector, we create their monthly climatologies. The climatological density profiles are calculated from the averaged T and S climatologies using the TEOS equation (McDougall & Barker, 2011). From these climatologies, the vertical gradient of temperature (dT/dz), density (dp/dz), and mixed layer depth (MLD) defined by an increase in density by 0.03 kg m^{-3} from the surface ocean density are calculated.

3. Results

3.1. Sea Ice Predictability-Summer Persistence and Spring Reemergence

Our analysis of sea ice and ocean predictability is in the forward-looking perspective that is indicating how a given initial state relates to future states. Sea ice area predictability results from observations and model data are similar (Figures 1b and 1c), and show two predictability patterns: “persistence” from summer initial months with correlations lasting till June, shown by a sustained significant autocorrelation (Figure 1c *) and ‘reemergence’ from spring initial months to the following autumn months (Figure 1c **), shown by the loss of correlation in

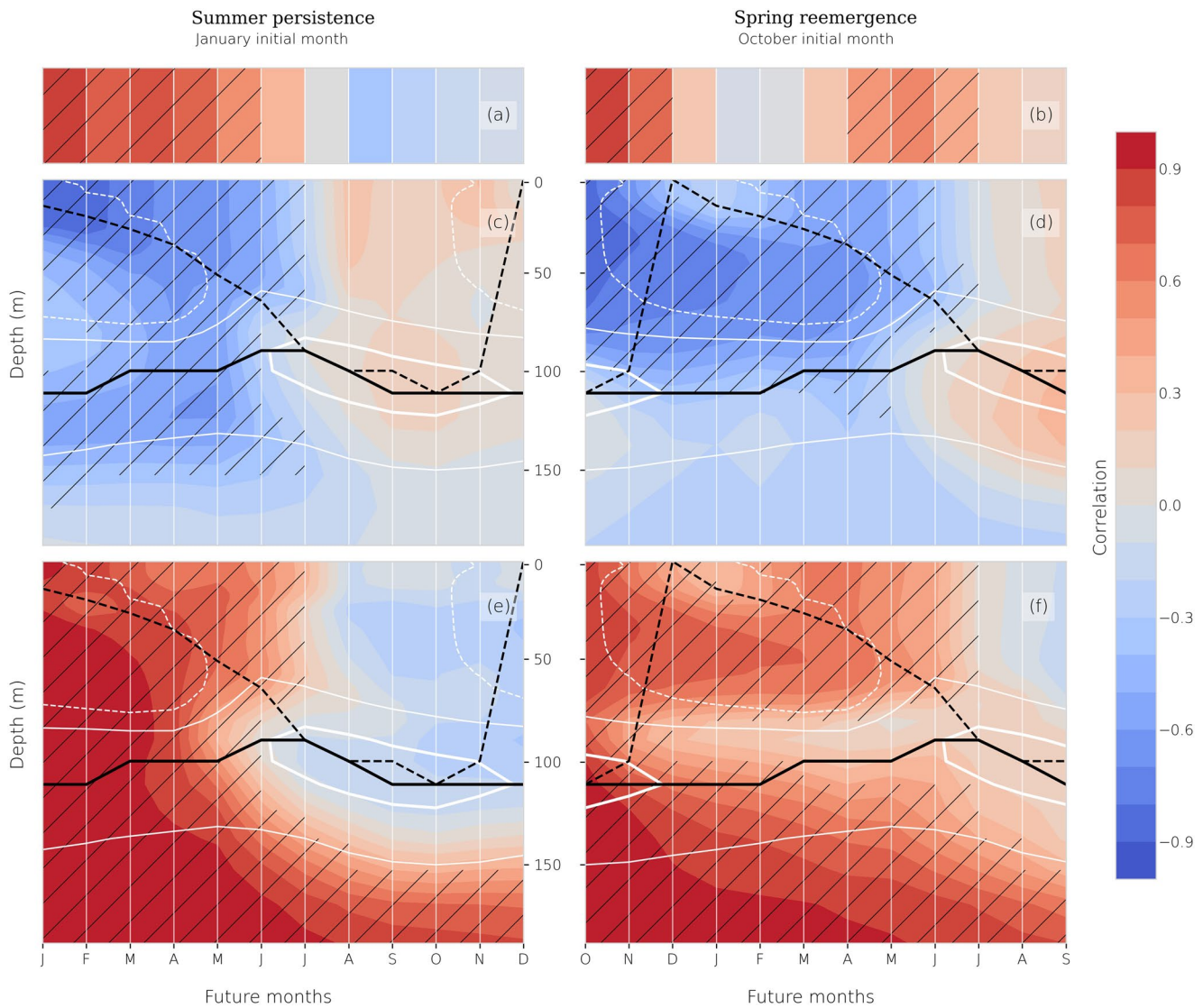


Figure 2. Comparison of summer persistence (plots on the left) and spring reemergence patterns (plots on the right) evident from sea ice (top row) and upper ocean predictability (0–200 m) (middle and bottom row). Sea ice predictability, correlation of sea ice area (SIA) from January (a) and October (b) initial months with future months; correlation between SIA in (c) January and (d) October with ocean temperature in future months; and correlation of ocean temperature in (e) January and (f) October with future months. Statistically significant values (>95%) are hatched in all panels. In the oceanic predictability results (c–f), the thick black line is the vertical temperature gradient (dT/dz) maximum, the dashed black line is the vertical density gradient (dp/dz) maximum, white contours are dT/dz contours, and white dashed contours bound the dT/dz values that are negative during summer stratification.

summer months, which ‘reemerges’ in April. These patterns of persistence in summer and reemergence from spring to autumn (hereafter “spring reemergence”) were identified in a similar diagnostic study by Ordoñez et al., 2018. Prognostic studies have identified the reemergence of Antarctic sea ice predictability during the ice-growth season (M. M. Holland et al., 2013; Marchi et al., 2019; Zunz et al., 2015). Our sea ice predictability results show the termination of both summer persistence and spring reemergence consistently occurring in July.

3.2. Ocean-Ocean and Ice-Ocean Correlations

The physical processes in the ocean underlying sea ice predictability patterns are investigated using the evolution of upper ocean predictability (Figure 2). We choose SIA correlations starting from January and October to represent summer persistence and spring reemergence patterns, respectively (Figures 2a and 2b). We correlate January and October SIA with lagged ocean temperature to explore how sea ice anomalies are related to upper ocean

temperature (ice-ocean correlation) (Figures 2c and 2d); the ocean's internal predictability is characterized by correlating the January and October temperature with future temperature at the same depth (ocean-ocean correlation) (Figures 2e and 2f). We find a consistent evolution of predictability between the three sets of correlations. Sea ice and ocean autocorrelations (Figures 2a, 2b, 2e, and 2f) are positive, whereas ice-ocean correlations are negative, since cooler temperature implies more ice.

3.2.1. Seasonal Evolution of the Upper Ocean

We overlay the climatological vertical thermal and density gradient contours to follow the seasonal evolution of the water column. The climatological dT/dz maximum (black line) represents the permanent pycnocline (PP) that separates the Winter Water (WW; i.e., cold water formed during sea ice production and its summer remnant) from slowly modifying Circumpolar Deep Water (CDW). The dp/dz maximum (dashed black line) represents the evolution of seasonal pycnocline, which forms the base of the seasonally evolving mixed layer that is in direct exchange with the surface. Seasonal pycnocline acts as the base of mixed layer in summer (January–March) and autumn (April–June), before it merges with the PP in winter (more information in Supporting Information S1 [Text S1 and Figure S2]).

During the ice growth season, the PP coincides with the maximum depth of statistically significant correlations (Figure 2d). There is a layer of weak correlations at the base of the WW (Figure 2f), which we interpret as noise, due to the high variability from mixing processes at the interface of the upper ocean and ocean interior. This separation (weak correlations) at the base of WW is expected, since WW is modified by sea ice production, implying that the entire WW is a source of memory for the ice-ocean system. The high correlations below the PP in the ocean-ocean correlations (below ~ 150 m depth, Figures 2e and 2f) are linked to the longer variance timescale of deep waters compared to surface waters, but are not associated with sea ice variability. Therefore, in our paper, we focus mainly on the predictability evolving in the upper ocean (top 100 m, Figures 2c–2f) largely within the WW layer to evaluate the physical processes in the ocean that influence sea ice predictability.

3.2.2. Freeze and Melt as Limits to Predictability

The correlations emerging from October encounter the loss of predictability during summer lag months and present predictability reemergence (Figures 2b, 2d, and 2f). Consistent with M. M. Holland et al. (2013) and Marchi et al. (2019), the oceanic predictability shows the weakening or loss of correlations during summer near the surface, while strong correlations are retained below this surface layer and above the PP. Freshwater and surface ocean warming during the ice melt season (December–February) produce a thin and highly stratified surface layer that becomes the summer mixed layer (dashed black line) in Figures 2c–2f. This summer layer separates the thermal anomalies in the WW layer from the surface, causing the loss of predictability between December and March (Figures 2b, 2d, and 2f).

In March, the regime shifts from sea ice melt (and a well-stratified summer mixed layer) to sea ice production (and destratification at the surface). Brine rejection from sea ice growth induces vertical mixing, resulting in entrainment across the seasonal mixed layer. Initially, this entrainment reconnects the relatively cold remnant WW layer with the surface layer, leading to the reemergence of both sea ice and ocean predictability (M. M. Holland et al., 2013; Marchi et al., 2019). After entraining through the WW layer, the mixed layer continues to deepen, eventually reaching the PP (merging of dashed black line with black line in Figures 2c–2f). Further entrainment causes the loss of predictability (Figure 1c and all panels of Figure 2), as it entrains water that has no sea ice process-related memory. We call this loss in predictability the “predictability barrier,” which is discussed in Section 4.1.

3.2.3. Sensitivity of Sea Ice Predictability to the Stratification Strength at the Base of the Winter Water Layer

The main distinction between ice-ocean correlations and ocean-ocean correlations is that ice-ocean correlations are largely bounded by the PP (upper 100 m), while the ocean-ocean correlations produce significant correlations below the PP (below 100 m). As discussed in Section 3.2.1, ice-ocean correlations emerging from October are bounded by the PP, which we attribute to the sea ice memory being confined to the WW. However, the January SIA is correlated with ocean temperatures below the PP (up to 150 m; Figure 2c). Here, we put forward the hypothesis that this is due to changes in the strength of the stratification at the base of the WW (or at the PP) (Figure 3e).

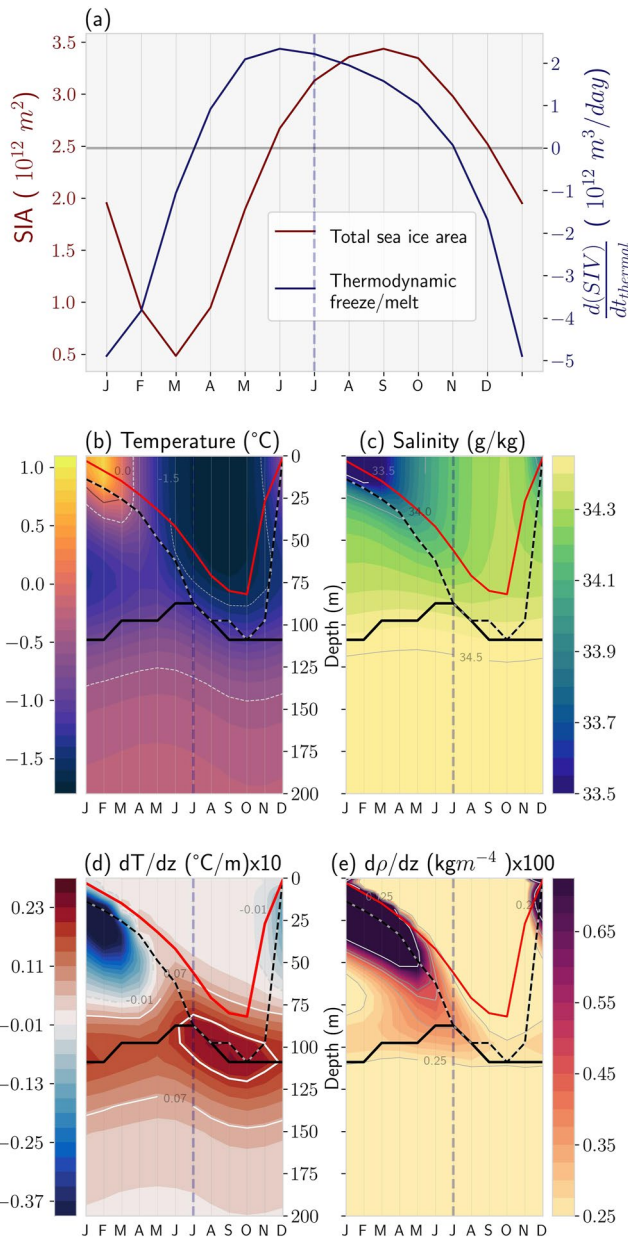


Figure 3. Annual evolution of climatological (a) sea ice area (red line) and thermodynamic freeze and melt (blue line), (b) temperature, (c) salinity, (d) vertical temperature gradient (dT/dz), and (e) vertical density gradient ($d\rho/dz$), spatially averaged over the sea ice covered ocean zone of the Weddell sector in the upper 200 m. The vertical temperature gradient maximum (thick black line), vertical temperature gradient (white lines), and vertical density gradient maximum (dashed line) are the same used in Figure 2 and mixed layer depth (red line) is marked on all panels.

Winter cooling and sea ice production create a WW layer that is very distinct from CDW, which maintains a strong PP; therefore, the sea ice memory is confined above PP. Stratification strength at the PP reaches its maximum immediately before the occurrence of the predictability barrier in July, following which the PP stratification weakens due to entrainment-driven mixing across the PP, reaching its minimum in spring (by October, Figure 3e). Ice-ocean correlations for all 12 initial months (Figure S1 in Supporting Information S1) show how the correlations respond to changes in stratification strength. The correlations initialized from November to May (i.e., when the PP is weakest) extend below the PP, but otherwise correlations are bounded by the PP. This suggests that the strength of the PP, which itself is modified by sea ice growth/brine rejection (and related mixing of the CDW and WW), is an important indicator for how well heat anomalies are retained in the sea ice-mixed layer system. Doddridge et al. (2021) demonstrated that during the ice melt season, turbulent mixing can move heat anomalies downward across the summer mixed layer and into the remnant WW layer; here, we posit a similar process happening before the development of the summer mixed layer, so that temperature anomalies penetrate below the PP. In this case, the memory from those thermal anomalies is lost to the CDW (which acts as a thermal sink).

Importantly, this variability in the depth of significant correlation (Figures 2c and 2d) demonstrates that the strength of stratification, as well as the depth, of the PP is important for the regime of sea ice predictability in a given sector. We further discuss the dependence of sea ice predictability on the hydrographic profile in Section 4.2.

4. Discussions

4.1. Predictability Barrier and Predictability Suppression

Our study is consistent with findings from existing literature connecting upper OHC (oceanic thermal memory) with sea ice predictability (M. M. Holland et al., 2013; Marchi et al., 2019; Ordoñez et al., 2018; Zunz et al., 2015). In the Weddell Sea, sea ice anomalies persisting from spring are lost temporarily in summer (December–May) and then reemerge in May before they are lost permanently in mid-winter (July) (Figure 2, all panels). Seasonal loss of sea ice predictability (in summer) is associated with the development of a highly stratified summer mixed layer due to sea ice melt that separates the surface ocean and sea ice from the heat content anomalies below the summer mixed layer. Below the summer mixed layer, OHC anomalies are retained and reemerge when the summer mixed layer erodes and deepens in autumn. This is consistent with the reemergence mechanism explained by M. M. Holland et al. (2013) and Marchi et al. (2019).

After reemerging, predictability is suddenly lost in mid-winter (in July). The loss in predictability is consistent among all three sets of correlation analysis. We call this loss in predictability as the “predictability barrier.” In our analysis, the predictability barrier is a clear, sharp loss of correlations in July (regardless of the lead month) and not the gradual decline we might expect

from statistical red noise. This implies that there is a change in the physical system in July. Previous studies (Blanchard-Wrigglesworth et al., 2011; Giesse et al., 2021; Ordoñez et al., 2018) also show the permanent loss of predictability on a specific month (or a set of months in the same season), but they do not explain the physical mechanism of this barrier.

Since predictability arises from OHC in the mixed layer, loss of predictability suggests the modification of OHC within the mixed layer. The changes in OHC causing the loss of predictability in mid-winter can be caused by the mixed layer losing heat to the atmosphere as it cools the upper ocean and produces sea ice or as the mixed layer gains heat from the ocean interior. The climatological sea ice freezing rate (Figure 3a) shows no sudden increase, suggesting there are no sudden changes in ocean-atmosphere fluxes that could explain a sudden loss of predictability. In Section 3.2, we have shown that the predictability barrier coincides with the time at which the seasonal pycnocline merges with PP. During the ice growth season, the atmosphere cools the upper ocean inducing sea ice growth, and deepening the mixed layer through enhanced vertical mixing from the brine released. Initially, this entrains remnant WW containing sea ice memory into the mixed layer, which explains the reemergence of predictability. Once the mixed layer deepens to reach the PP, further sea ice growth entrains heat from the ocean interior (CDW) into the mixed layer (Gordon & Huber, 1984, 1990; Martinson, 1990; Wilson et al., 2019), which has no sea ice-related memory, therefore terminating predictability.

Martinson (1990) and Wilson et al. (2019) showed that vertical heat flux driven by brine rejection placed a constraint on winter sea ice growth. Our analysis shows that this constraint is likely invoked in mid-winter in the Weddell sector, when warm CDW is entrained into the mixed layer. The timing of predictability barrier signals when the negative ice-ocean feedback limiting ice growth rate due to entrainment is activated.

Goosse and Zunz (2014) and Lecomte et al. (2017) showed how increased stratification in the upper ocean reduced the vertical heat flux from CDW during ice growth, which enabled positive ice-ocean feedbacks. Lecomte et al. (2017) found the positive ice-ocean feedback associated with a long-term trend in SIC only in the Ross sector. The fact that they do not find positive ice-ocean feedback in the Weddell Sea is consistent with our finding of the existence of a predictability barrier that prevents the persistence of anomalies beyond 12 months. Therefore, the existence of this predictability barrier is a consequence of the absence of near-surface ice-ocean feedbacks that could potentially lead to long-term trends (in upper ocean properties and SIC). By investigating regional Antarctic sea ice predictability, one can determine the presence or absence of predictability barriers that will provide valuable insights into long-term sea ice trends.

4.2. Dependence of Sea Ice Predictability on Mixed Layer Depth/ Winter Water Layer Depth

The mixed layer depth (MLD) has been given high relevance in previous studies of sea ice predictability. M. M. Holland et al. (2013) and Marchi et al. (2019) observed spatial variability in their prognostic sea ice predictability analysis and suggested that sufficiently deep mixed layers were required for retaining heat anomalies and hosting sea ice predictability. Our results align closely with findings from Marchi et al. (2019) in that the temperature anomalies relevant to sea ice predictability are stored at the depth range typical of WW. However, as discussed in Section 3.2.2, we find instances where, the depth to which temperature anomalies extends vary depending on the stratification strength at the PP. When the stratification is weak, the T anomalies (memory) extend deeper than the WW. Also, Marchi et al. (2019) suggested that the effectiveness of the reemergence mechanism is associated with a sufficiently large seasonal cycle of MLD (i.e., a transition from a shallow highly stratified summer mixed layer to the deep WW). However, Ordoñez et al. (2018) suggested that the variable MLD is less important to sea ice predictability than basic mixed layer temperature persistence, suggesting that the MLD is not the only important criterion for sea ice predictability during ice melt and growth season.

By using the maximum density gradient for evaluating the upper ocean evolution against MLD in our study, we were able to identify a physical constraint (predictability barrier) on sea ice predictability. This shows that it is not simply the depth to which the anomalies extend in the WW or ML that determines the potential for sea ice predictability, but also how well the thermal signatures linked to sea ice processes are retained in the upper ocean. The predictability barrier occurs with the transfer of anomalies (thermal signatures) across the PP, implying that the water across the PP is overcoming the “barrier” of maximum stratification in the upper ocean. Our key finding is that sea ice and its underlying oceanic predictability follow changes in vertical ocean structure (dT/dz and dp/dz gradients; Figure 2, all panels). Therefore, the vertical ocean structure in any region and its modification via sea ice processes determine its potential for retaining oceanic thermal memory, and by focusing only on the MLD, we lose other key features and processes related to sea ice predictability and its spatial variability.

Our sea ice predictability analysis has produced results consistent with previous studies; however, we take caution while comparing our results with the earlier studies: (a) we use a coupled ocean-sea ice model driven by

reanalysis atmospheric fields, while previous Antarctic sea ice predictability studies (M. M. Holland et al., 2013; Marchi et al., 2019; Ordoñez et al., 2018; Zunz et al., 2015) used coupled atmosphere-ocean-sea ice models and (b) the regional diagnostic (using lagged correlations) sea ice predictability analysis in our study is similar to Ordonez et al. (2018), while other studies use prognostic methods (using model ensemble spread). The coupled ocean-sea ice model provides a fair representation of the ice-ocean system required for our analysis at the spatial and temporal scales used in our study. The effect of atmospheric coupling would be important if the atmosphere responded significantly to sea ice variability; however, previous work (England et al., 2018; M. Raphael et al., 2011) suggested this is not true at the spatial scales that we consider here.

Our analysis looks at changes in total SIA and ocean properties averaged over a large area in the Weddell Sea. The oceanic domain is also time-fixed since the uptake of solar energy in open water (within sea ice zone as ice melts back) is an important source of summer-autumn predictability through ice-albedo feedbacks (Stammerjohn et al., 2012). Spatial plots of the variation in temperature, dT/dz and dp/dz (Figures S3 and S4 in Supporting Information S1), reveal two regimes, (a) the approximate “2-layer” system that dominates our correlations and (b) a narrow band of destratification (indicating Dense Shelf Water production) near the Ronne ice shelf. The destratified region does not show large seasonal changes (especially below 50 m), whereas in the 2-layer system, the vertical gradients evolve closely aligning with the averaged climatological profiles in Figure 3. Figures S5 and S6 in Supporting Information S1 reveal that the SIA is affected largely by sea ice variability in the 2-layer system, more information and discussion in Supporting Information S1 (Text S2).

We also do not consider the variability within the region, such as the transport of sea ice nor the advection of oceanic properties. Sea ice motion can transport ice in or out of the sector or move it within the sector. Our estimate from the model shows that ~92% of the sea ice that forms in the Weddell sector melts within it; hence, in a bulk scale, the net dynamic term is minimal compared to thermodynamic freeze/melt. Sea ice motion driven by the atmosphere and the ocean (primarily the Weddell gyre) impacts predictability by reducing the skill. Ice motion dominated by synoptic variability is inherently “unpredictable” at the monthly-to-seasonal timescales that we consider here; Oceanic advection, especially strong northward drift, reduces predictability skill (Bushuk et al., 2021; M. M. Holland et al., 2013). There may also be some relationship between sea ice variability and the strength of Weddell gyre (Neme et al., 2021) potentially impacting sea ice predictability. However, that is a complex relationship beyond the focus of this analysis. By averaging over a larger area such that thermodynamic effects become more important, we can see the predictability that arises from upper ocean heat storage (ocean memory), and the problem becomes tractable.

We have relied solely on the correlations to draw our interpretations and use the climatological oceanic parameters to guide our arguments. Quantifying the seasonal exchanges and thermal modifications occurring in the upper ocean is a potential follow-up analysis.

5. Conclusions

Over the 40 years of satellite record of Antarctic sea ice, the last decade has seen particularly large fluctuations in sea ice extent, including a record high value in 2014 followed by a record low in 2016–2017. These recent fluctuations and the uncertainties in sea ice variability and trends linked to climate change make the emerging field of sea ice prediction particularly relevant. In this study, we have analyzed the predictability of sea ice and underlying ocean in the Weddell sector of the Southern Ocean using lagged correlations. We find that (a) sea ice predictability emerging from summer months persists until mid-winter and (b) sea ice predictability emerging from spring months has a temporary loss during summer months and reemerges in autumn months. We also find that the predictability in the ocean linked to sea ice predictability is largely confined to the Winter Water layer, and it is dependent not only on the depth of the Winter Water layer but also heavily controlled by changes in the strength of stratification at the base of the Winter Water layer. Therefore, both these hydrographic parameters may be valuable for understanding regional differences in Antarctic sea ice trends and variability.

Our results are consistent with M. M. Holland et al. (2013) and Marchi et al. (2019) in (a) connecting the OHC with sea ice predictability and (b) with their proposed mechanism of predictability reemergence. In addition to the temporary loss of predictability in summer lag months prior to predictability reemergence, we find a more permanent loss of predictability in mid-winter. In mid-winter, when the seasonal pycnocline merges with the PP, warm CDW with no sea ice-related memory entrains into the mixed layer and terminates the predictability. The

key insights from our study are in finding that (a) regional sea ice predictability is tied to the vertical structure of its oceanic properties and how this structure evolves, especially when forced by sea ice processes. This implies that the spatial variability in sea ice predictability can now be addressed based on local upper ocean vertical structure and sea ice processes. We also find that (2) the strength of stratification at the base of the Winter Water layer is relevant in determining potential sea ice predictability.

Oceanic predictability can be summed up as thermal anomalies lingering in the ice-ocean system at interannual timescales. These thermal anomalies generate sea ice predictability, which implies that sea ice predictability is a signature of local ice-ocean interaction mediated by residual thermal anomalies. Therefore, our analysis not only improves our knowledge and capacity for operational Antarctic sea ice forecast, but it also presents a potential tool for evaluating the regional signature of ice-ocean interactions. The fact that sea ice predictability is strongly tied to the vertical structure of oceanic properties suggests that changes in the upper ocean in a warming climate are likely to alter Antarctic sea ice predictability patterns in the future.

Data Availability Statement

All model outputs including the simulations presented in this manuscript is stored as part of the COSIMA data collection (<https://doi.org/10.4225/41/5a2dc8543105a>). Passive microwave sea ice data are publicly available, hosted by the National Snow and Ice Data Center (<https://doi.org/10.7265/N59P2ZTG>).

References

- Abernathy, R. P., Cerovecki, I., Holland, P. R., Newsom, E., Mazloff, M., & Talley, L. D. (2016). Water-mass transformation by sea ice in the upper branch of the Southern Ocean overturning. *Nature Geoscience*, 9, 596–601. <https://doi.org/10.1038/ngeo2749>
- Blanchard-Wrigglesworth, E., Armour, K. C., Bitz, C. M., & De Weaver, E. (2011). Persistence and inherent predictability of Arctic Sea ice in a GCM ensemble and observations. *Journal of Climate*, 24(1), 231–250. <https://doi.org/10.1175/2010jcli3775.1>
- Brandt, R. E., Warren, S. G., Worby, A. P., & Grenfell, T. C. (2005). Surface albedo of the Antarctic sea ice zone. *Journal of Climate*, 18(17), 3606–3622. <https://doi.org/10.1175/jcli3489.1>
- Bushuk, M., Winton, M., Haumann, F. A., Delworth, T., Lu, F., Zhang, Y., et al. (2021). Seasonal prediction and predictability of regional Antarctic sea ice. *Journal of Climate*, 1–68. <https://doi.org/10.1175/jcli-d-20-0965.1>
- Chen, D., & Yuan, X. (2004). A Markov Model for seasonal forecast of Antarctic sea ice. *Journal of Climate*, 17(16), 3156–3168. [https://doi.org/10.1175/1520-0442\(2004\)017<3156:Ammfsf>2.0.Co;2](https://doi.org/10.1175/1520-0442(2004)017<3156:Ammfsf>2.0.Co;2)
- Doddridge, E. W., Marshall, J., Song, H., Campin, J.-M., & Kelley, M. (2021). Southern Ocean heat storage, reemergence, and winter sea ice decline induced by summertime winds. *Journal of Climate*, 34(4), 1403–1415. <https://doi.org/10.1175/jcli-d-20-0322.1>
- England, M., Polvani, L., & Sun, L. (2018). Contrasting the Antarctic and Arctic atmospheric responses to projected sea ice loss in the late twenty-first century. *Journal of Climate*, 31(16), 6353–6370. <https://doi.org/10.1175/jcli-d-17-0666.1>
- Giesse, C., Notz, D., & Baehr, J. (2021). On the origin of discrepancies between observed and simulated memory of Arctic Sea ice. *Geophysical Research Letters*, 48(11), e2020GL091784. <https://doi.org/10.1029/2020GL091784>
- Goosse, H., & Zunz, V. (2014). Decadal trends in the Antarctic sea ice extent ultimately controlled by ice-ocean feedback. *The Cryosphere*, 8(2), 453–470. <https://doi.org/10.5194/tc-8-453-2014>
- Gordon, A. L., & Huber, B. A. (1984). Thermohaline stratification below the Southern Ocean sea ice. *Journal of Geophysical Research*, 89(C1), 641–648. <https://doi.org/10.1029/jc089ic01p00641>
- Gordon, A. L., & Huber, B. A. (1990). Southern ocean winter mixed layer. *Journal of Geophysical Research*, 95(C7), 11655. <https://doi.org/10.1029/jc095ic07p11655>
- Guemas, V., Chevallier, M., Déqué, M., Bellprat, O., & Doblas-Reyes, F. (2016). Impact of sea ice initialization on sea ice and atmosphere prediction skill on seasonal timescales. *Geophysical Research Letters*, 43(8), 3889–3896. <https://doi.org/10.1002/2015gl066626>
- Handcock, M. S., & Raphael, M. N. (2020). Modeling the annual cycle of daily Antarctic sea ice extent. *The Cryosphere*, 14(7), 2159–2172. <https://doi.org/10.5194/tc-14-2159-2020>
- Hobbs, W. R., Massom, R., Stammerjohn, S., Reid, P., Williams, G., & Meier, W. (2016). A review of recent changes in Southern Ocean sea ice, their drivers and forcings. *Global and Planetary Change*, 143, 228–250. <https://doi.org/10.1016/j.gloplacha.2016.06.008>
- Holland, M. M., Blanchard-Wrigglesworth, E., Kay, J., & Vavrus, S. (2013). Initial-value predictability of Antarctic sea ice in the Community Climate System Model 3. *Geophysical Research Letters*, 40(10), 2121–2124. <https://doi.org/10.1002/grl.50410>
- Holland, P. R. (2014). The seasonality of Antarctic sea ice trends. *Geophysical Research Letters*, 41(12), 4230–4237. <https://doi.org/10.1002/2014gl060172>
- Juricke, S., Goessling, H. F., & Jung, T. (2014). Potential sea ice predictability and the role of stochastic sea ice strength perturbations. *Geophysical Research Letters*, 41(23), 8396–8403. <https://doi.org/10.1002/2014gl062081>
- Kearney, K. A., Alexander, M., Aydin, K., Cheng, W., Hermann, A. J., Hervieux, G., & Ortiz, I. (2021). Seasonal predictability of sea ice and bottom temperature across the eastern Bering Sea Shelf. *Journal of Geophysical Research: Oceans*, 126(11), e2021JC017545. <https://doi.org/10.1029/2021JC017545>
- Kiss, A. E., Hogg, A. M., Hannah, N., Boeira Dias, F., Brassington, G. B., Chamberlain, M. A., et al. (2020). ACCESS-OM2 v1.0: A global Ocean-sea ice model at three resolutions. *Geoscientific Model Development*, 13(2), 401–442. <https://doi.org/10.5194/gmd-13-401-2020>
- Lecomte, O., Goosse, H., Fichefet, T., Barthélemy, A., De Lavergne, C., & Zunz, V. (2017). Vertical ocean heat redistribution sustaining sea-ice concentration trends in the Ross Sea. *Nature Communications*, 8(1), 258. <https://doi.org/10.1038/s41467-017-00347-4>

Acknowledgments

This project received grant funding from the Australian Government as part of the Antarctic Science Collaboration Initiative program. The Australian Antarctic Program Partnership is led by the University of Tasmania and includes the Australian Antarctic Division, CSIRO Oceans and Atmosphere, Geoscience Australia, the Bureau of Meteorology, the Tasmanian State Government, and Australia's Integrated Marine Observing System. SL and AM acknowledge support from the Australian Research Council Center of Excellence for Climate Extremes (CE170100023). A. Meyer was supported by the Australian Research Council Discovery Early Career Research Award project DE200100414. S. Libera acknowledges Quantitative Marine Science (QMS) research scholarship (including support from the CSIRO Post-graduate scheme), University of Tasmania tuition fee scholarship. This research was undertaken with the assistance of resources from the National Computational Infrastructure (NCI), which is supported by the Australian government. We thank the Consortium for Ocean-Sea Ice Modeling in Australia (COSIMA; www.cosima.org.au), funded by the Australian Research Council through its Linkage Program (LP160100073), for making the ACCESS-OM2 suite of models available. Open access publishing facilitated by University of Tasmania, as part of the Wiley - University of Tasmania agreement via the Council of Australian University Librarians.

- Marchi, S., Fichefet, T., & Goosse, H. (2020). Respective influences of perturbed atmospheric and ocean–Sea ice initial conditions on the skill of seasonal Antarctic Sea ice predictions: A study with NEMO3.6–LIM3. *Ocean Modelling*, *148*, 101591. <https://doi.org/10.1016/j.ocemod.2020.101591>
- Marchi, S., Fichefet, T., Goosse, H., Zunz, V., Tietsche, S., Day, J. J., & Hawkins, E. (2019). Reemergence of Antarctic sea ice predictability and its link to deep ocean mixing in global climate models. *Climate Dynamics*, *52*(5), 2775–2797. <https://doi.org/10.1007/s00382-018-4292-2>
- Martinson, D. G. (1990). Evolution of the southern ocean winter mixed layer and sea ice: Open ocean deepwater formation and ventilation. *Journal of Geophysical Research*, *95*(C7), 11641–11654. <https://doi.org/10.1029/JC095iC07p11641>
- Massom, R. A., & Stammerjohn, S. E. (2010). Antarctic sea ice change and variability—Physical and ecological implications. *Polar Science*, *4*(2), 149–186. <https://doi.org/10.1016/j.polar.2010.05.001>
- Massonnet, F., Reid, P., Lieser, J., Bitz, C., Fyfe, J., & Hobbs, W. (2019). *Assessment of summer 2018–2019 sea-ice forecasts for the Southern Ocean*.
- McDougall, T. J., & Barker, P. M. (2011). Getting started with TEOS-10 and the Gibbs Seawater (GSW) oceanographic toolbox. *SCOR/IAPSO WG*, *127*, 1–28.
- Meier, W. N., Fetterer, F., Savoie, M., Mallory, S., Duerr, R., & Stroeve, J. (2013). NOAA/NSIDC climate data record of passive microwave sea ice concentration. Retrieved from https://nsidc.org/data/docs/noaa/g02202_ice_conc_cdr/
- Neme, J., England, M. H., & Hogg, A. M. (2021). Seasonal and interannual variability of the Weddell Gyre from a high-resolution global ocean-sea ice simulation during 1958–2018. *Journal of Geophysical Research: Oceans*, *126*(11), e2021JC017662. <https://doi.org/10.1029/2021jc017662>
- Ordoñez, A. C., Bitz, C. M., & Blanchard-Wrigglesworth, E. (2018). Processes controlling Arctic and Antarctic sea ice predictability in the Community Earth System Model. *Journal of Climate*, *31*(23), 9771–9786. <https://doi.org/10.1175/jcli-d-18-0348.1>
- Raphael, M., Hobbs, W., & Wainer, I. (2011). The effect of Antarctic sea ice on the Southern Hemisphere atmosphere during the southern summer. *Climate Dynamics*, *36*(7), 1403–1417. <https://doi.org/10.1007/s00382-010-0892-1>
- Raphael, M. N., & Hobbs, W. (2014). The influence of the large-scale atmospheric circulation on Antarctic sea ice during ice advance and retreat seasons. *Geophysical Research Letters*, *41*(14), 5037–5045. <https://doi.org/10.1002/2014gl060365>
- Simpkins, G. R., Ciaso, L. M., Thompson, D. W., & England, M. H. (2012). Seasonal relationships between large-scale climate variability and Antarctic sea ice concentration. *Journal of Climate*, *25*(16), 5451–5469. <https://doi.org/10.1175/jcli-d-11-00367.1>
- Stammerjohn, S., Massom, R., Rind, D., & Martinson, D. (2012). Regions of rapid sea ice change: An inter-hemispheric seasonal comparison. *Geophysical Research Letters*, *39*(6). <https://doi.org/10.1029/2012gl050874>
- Tsujino, H., Urakawa, S., Nakano, H., Small, R. J., Kim, W. M., Yeager, S. G., et al. (2018). JRA-55 based surface dataset for driving ocean–sea-ice models (JRA55-do). *Ocean Modelling*, *130*, 79–139. <https://doi.org/10.1016/j.ocemod.2018.07.002>
- Wilson, E. A., Riser, S. C., Campbell, E. C., & Wong, A. P. S. (2019). Winter upper-ocean stability and ice–ocean feedbacks in the sea ice–covered Southern Ocean. *Journal of Physical Oceanography*, *49*(4), 1099–1117. <https://doi.org/10.1175/jpo-d-18-0184.1>
- Yang, C.-Y., Liu, J., Hu, Y., Horton, R. M., Chen, L., & Cheng, X. (2016). Assessment of Arctic and Antarctic sea ice predictability in CMIP5 decadal hindcasts. *The Cryosphere*, *10*(5), 2429–2452. <https://doi.org/10.5194/tc-10-2429-2016>
- Zampieri, L., Goessling, H. F., & Jung, T. (2019). Predictability of Antarctic sea ice edge on subseasonal time scales. *Geophysical Research Letters*, *46*(16), 9719–9727. <https://doi.org/10.1029/2019gl084096>
- Zunz, V., Goosse, H., & Dubinkina, S. (2015). Impact of the initialisation on the predictability of the Southern Ocean sea ice at interannual to multi-decadal timescales. *Climate Dynamics*, *44*(7–8), 2267–2286. <https://doi.org/10.1007/s00382-014-2344-9>